Elsevier Editorial System(tm) for Journal of Atmospheric and Solar-Terrestrial Physics

Manuscript Draft

Manuscript Number: ATP1526R1

Title: Day-by-day modelling of the ionospheric F2-layer for year 2002

Article Type: Research Paper

Keywords: Ionospheric modeling; General Circulation Models; Model-Data Comparisons; F-layer Morphology

Corresponding Author: Miss Joei Wroten, B.S.

Corresponding Author's Institution: Boston University

First Author: Henry Rishbeth, Ph.D

Order of Authors: Henry Rishbeth, Ph.D; Michael Mendillo, Ph.D; Joei Wroten, B.S.; Raymond Roble, Ph.D

Abstract: The Thermosphere-Ionosphere-Mesosphere-Electrodynamics General Circulation Model (TIME-GCM) has been run for the year 2002. Its version 1.2 features include day-by-day input of solar irradiance, geomagnetic energy input parameterized by the 3-hour Kp index, and global lower boundary conditions from the National Centres for Environmental Predictions (NCEP) data. In addition it includes tidal forcing from the Global Scale Wave Model and parameterized gravity waves from below. The computed day-by-day values of noon peak electron density NmF2 agree well with ionosonde data for five northern sites and two southern mid-latitude sites, and closely follow the day-by-day modelled concentration ratio of atomic oxygen to molecular nitrogen. Seasonal and hemispheric patterns appear in the model with some, though not full, success. The model's day-to-day patterns show an impressive degree of variability, with simulations of total variability both above and below those observed.

ATP1526_Reply to Referee Comments – Prepared by Rishbeth 24 Dec 2008

Note to Editor and Referees: We have made very major changes to the text, tables and the ordering of the figures. Trying to show these with some color-coding, or the use of a different type style to show them, turned out to be a most un-useful aid in that there are nearly more changes than original material! We appreciate the thoughtful suggestions and comments that led to these major revisions.

With respect, we strongly disagree with Referee 1 that our paper ref ATP1526 is no advance on our 2002 paper. True, we use the same seven stations. But there is a great difference between the inputs. The 2002 paper used month-by-month averages of an 'idealized year' with fixed solar flux and magnetic activity, while the new paper uses the actual day-by-day variations in year 2002, a much more challenging task, and compares them with the actual F2-layer variations at these stations.

We also question Ref 1's assertion that "many papers using models based on MSIS, as well as coupled models, have generated this [the annual anomaly]. In this writer's opinion [Rishbeth], there is a great difference between an *empirical* model like MSIS, in which the parameters are computed in order to reproduce the experimental and observational data that show such features as the annual anomaly, and computational models [sometimes called 'first principles models'] that are constructed by numerically solving the basic conservation equations for mass, momentum, energy. Rightly or wrongly, Rishbeth & Mueller-Wodarg (2006) concluded that there existed no satisfactory explanation for the annual anomaly, other than the hypothesis of different north and south [or January and July] ionospheres. Subsequently, recent work at NCAR (quoted in the revised version) may have solved the problem, but does that constitute 'many publications'?

We admit that the original title and abstract failed to convey the great advance on our earlier paper, and hope that the new title and abstract rectify this. Specific Items:

MIDLAT Referee 1

Line 92. A reference justifying this adjustment [of eddy diffusion coefficient from 90 to 40 $m^2\ s^{-1}$] or text describing it should be given.

Reply: Qian et al. (2008), now in press with JGR is in the references, and its main result of an annual pattern is mentioned specifically.

Line 122. Figure 2 does not show all three Ap, Kp and |Dst| indices. Kp is missing hence "three panels" should be two.

Reply: We regret that one panel was wrongly labelled. This is now Figure 1 and is labelled correctly for the three panels it contains.

Line 89. The notation "c"-model. Is this the same as the earlier CCM3? If not, what distinguishes these two? Since to the best I can compare the two texts they are the same.

Reply: We agree that the model versions were not fully explained. This section has been re-written and we now use only the notation TIME-GCM-1.2 to distinguish this model from other versions. Version 1.1 was the one with CCM3 used in our earlier paper. The version used in this paper, as now explained extensively in the text, does not use CCM3.

Line 446. Figure 3 caption begins with "daytime" but the plot shows NmF2 at all local times.

Reply: Figures have been re-ordered and captions are corrected.

MIDLAT Referee 2

Line 187: It would be very useful to have a short discussion of the sensitivity of NmF2 to the O/N2 ratio and to the O+ flux to support the conclusion (line 236) "The key to success is correct representation of the neutral air composition in the thermosphere".

Reply: We have added to the paper a new section (3.4) dealing with seasonal-hemispheric patterns and the O/N2 ratios associated with them (new Figures 5, 6 and 7). In section 5.3 we specifically mention the ratios associated with successful data-model comparisons (i.e., those in the 3 to 9 domain).

Line 190: The high NmF2 values in winter in the South, caused by high O/N2 ratios, may be the result of a coherent downwelling that is concentrated in a small region. There is ample evidence that Joule heating at high latitudes involves small spatial scales (tens of km to hundreds of km) and time scales of seconds to minutes. The inclusion of the effects of such small scale processes results in an additional mixing of the atmosphere that may reduce the coherence of the downwelling (similar to an increase in eddy diffusion), reduce the O/N2 ratios and reduce the peak electron density.

Reply: We agree that the high O/N2 ratios are linked to a zone of downwelling in the sub-auroral winter hemisphere, as shown by the CTIPM computations, and discussed more fully in section 5.3. As the grid size of TIMEGCM does not allow study of smaller-scale processes, we cannot pursue the matter here. Thus, we have to assume that the increased eddy diffusion coefficient we now adopt [see Ref 1's remark concerning Line 92] is a reasonable way to represent the effect of such processes on the large-scale up/downwelling. This contrasts with Ref 1's complaint that 'no evidence for upwelling or downwelling is presented' [see our general remark about eddy diffusion above]. Also, we add to the paper a discussion of the Stratosphere warming effect that occurred in the southern hemisphere in 2002, with references dealing with it.

Note to Editor and Referees: We have made very major changes to the text, tables and the ordering of the figures. Trying to show these with some color-coding, or the use of a different type style to show them, turned out to be a most un-useful aid in that there are nearly more changes than original material! We appreciate the thoughtful suggestions and comments that led to these major revisions.

Day-by-day modelling of the ionospheric F2-layer for year 2002

H. Rishbeth[a,b] M. Mendillo[a], J. Wroten[a,*], R. G. Roble[c]

[a] Center for Space Physics, Boston University, 725 Commonwealth Avenue, Boston, MA 02215, U. S. A.

[b] School of Physics and Astronomy, University of Southampton, Southampton, SO17 1BJ, U. K.

[c] High Altitude Observatory, National Center for Atmospheric Research, Box 3000, Boulder, CO 80307, U. S. A.

rishbeth@soton.ac.uk, mendillo@bu.edu, jwroten@bu.edu, roble@hao.ucar.edu

Ref. ATP 1526_Revised by HR 15 Dec 2008

Abstract: The Thermosphere-Ionosphere-Mesosphere-Electrodynamics General Circulation Model (TIME-GCM) has been run for the year 2002. Its version 1.2 features include day-by-day input of solar irradiance, geomagnetic energy input parameterized by the 3-hour Kp index, and global lower boundary conditions from the National Centres for Environmental Predictions (NCEP) data. In addition it includes tidal forcing from the Global Scale Wave Model and parameterized gravity waves from below. The computed day-by-day values of noon peak electron density NmF2 agree well with ionosonde data for five northern sites and two southern mid-latitude sites, and closely follow the day-by-day modelled concentration ratio of atomic oxygen to molecular nitrogen. Seasonal and hemispheric patterns appear in the model with some, though not full, success. The model's day-to-day patterns show an impressive degree of variability, with simulations of total variability both above and below those observed.

* Corresponding Author. Center for Space Physics, Boston University, 725 Commonwealth Avenue, Boston, MA 02215, U. S. A. Tel:+00 1 617 353 2631; fax: +00-1-617-353-6463; E-mail address: jwroten@bu.edu

Keywords: Ionospheric modelling; General Circulation Models; Model-Data Comparisons; F-layer Morphology

1. Introduction

1.1 Background. The ionospheric F2-layer is well known to be highly variable. Most of its local-time, seasonal and solar-cycle variations are understood, in principle, and are thought to be largely caused by the global circulation in the thermosphere (Rishbeth, 1998). But the day-to-day and hour-to-hour variability of the layer are not well understood. Forbes et al. (2000), Fuller-Rowell et al. (2000) and Rishbeth and Mendillo (2001) attempted to evaluate the “solar EUV”, “geomagnetic” and “other” contributions to the day-to-day variability. The “other” component was tentatively attributed to so-called “meteorological” effects arising in the lower or middle atmosphere, but there is little firm observational evidence for this attribution. Before such contributions to variability can be evaluated via simulations that include these processes in ON/OFF modes, the basic global morphology of the ionosphere needs to be at a level of success worthy of such efforts. This is the goal of the current paper.

After listing in sections 1.2 and 1.3 the main objectives of the paper and new features of the approach used, we describe in section 2 the model and its inputs, compare in section 3 the model outputs with actual F2-layer data for seven sites, and discuss in section 4 the absolute numerical calibration against data of the noon values of NmF2. We discuss in section 5 the pattern of vertical flow of the neutral air – so-called ‘upwelling and downwelling’ – and summarize the conclusions in section 6.

We use here a recently updated version of the NCAR Thermosphere-Ionosphere-Mesosphere-Electrodynamics General Circulation Model (TIME-GCM version 1.2) which as before extends from the upper stratosphere at 28 km (10 hPa) to the base of the exosphere. At its lower boundary it is coupled to the daily-varying National Centres for Environmental Prediction (NCEP) climate data for the year 2002. The NCEP website is http://www.ncep.noaa.gov.

In our initial investigation of global model - data comparisons, Mendillo et al. (2002) used a much earlier version of TIME-GCM (1.1), coupled at its lower boundary to a version of the NCAR Community Climate Model (CCM3). In that work, coupling from above via solar and geomagnetic activity was held constant throughout the year, except for the geographic and seasonal changes of solar zenith angle. The results were therefore limited to the first exploration of model-data comparisons with a GCM that employed coupling from below in a model run for a full year. We discuss these limitations further in the following section.

1.2 Goals of this paper. We use here the TIME-GCM 1.2, and compare the modelled peak electron density NmF2 for every day of year 2002 with ionosonde data at seven mid-latitude sites. All three sources of daily variability are included, as compared to the approach described in Mendillo et al. (2002) for which only daily changes in forcing from below occurred. We concentrate on midday data, in order to evaluate the model under near photochemical equilibrium and provide some insight into the variability caused by solar and geomagnetic forcing, as well as coupling from the lower atmosphere. We consider the neutral atomic oxygen/molecular nitrogen concentration ratio (O/N_2) near the F2 peak resulting from all three sources. Our purpose, besides improving on the modelling presented in our previous paper as detailed in section 2.1, is to provide a basis for future work with different forcings imposed at the lower boundary.

In Mendillo et al. (2002), we used TIME-GCM-1.1 for a generic year of solar and geomagnetic activity, with CCM3 providing the daily coupling from below. Therefore, we could only assess seasonal trends with respect to ionosonde data that were also 'generic' – meaning we averaged several years of observations all having nearly the same solar F10.7 flux (of 140 units) as used in the model. The model had Ap = 4 for every day and auroral inputs set by cross polar cap potential = 45 kV and hemispheric power of 15 GW. Having sorted the ionosonde data only by F10.7, we had to take the average polar cap potential and hemispheric power for those years. We also described only the lower atmospheric variability from CCM3. We found both successes and discrepancies with the observed seasonal behaviour.

1.3 New features. The improvements offered in this new study are:

(a) A real year (2002) is used, both for the ionosonde data and for model drivers from above and below.

(b) CCM3 has been completely replaced by NCEP data at the lower boundary.

(c) The solar (F10.7) and the 3-hour geomagnetic activity (Kp) indices vary daily, so the parameterizations they drive for solar irradiance, the high latitude auroral power inputs and the ion convection patterns vary daily. Linear interpolation between daily or 3-hour indices is used to be compatible with the model time step.

(d) All aeronomic parameters (reaction rates and coefficients) have been updated to current values.

(e) The starting point for the thermosphere was adjusted by making the global mean match the MSIS -2000 (Picone et al., 2002) global mean for 2002. This required reducing the previously assumed value of the eddy diffusion coefficient from 90 to 45 $m^2 s^{-1}$, which changed the O/N_2 ratios, bringing the computed values of NmF2 closer to the ionosonde measurements.

(f) Some comparisons with TIE-GCM 1.9 were made while the paper was in revision, and these resulted in a change to the number of pressure levels used in TIMEGCM1.2, adding two pressure levels to the topside and therefore two more scale heights, which influenced the topside boundary condition, bringing the model into better agreement with ionosonde data.

(g) We conduct an evaluation of the hemispheric asymmetry in summer versus winter NmF2.

(h) With all three sources of variability included – solar, geomagnetic and upper stratospheric – the paper presents the first full-year modelling validation of ionospheric seasonal patterns at widely spaced midlatitude sites. While detailed assessment of total day-to-day F2-layer variability is reserved to a later paper, some preliminary observations on that key topic are made.

2. Model simulations for the year 2002.

2.1 Model Overview. The TIME-GCM (Thermosphere-Ionosphere-Mesosphere-Electrodynamics General Circulation Model) is a self-consistent coupled model of the upper stratosphere, mesosphere, thermosphere and ionosphere, incorporating aeronomic processes and dynamics with electrodynamic interactions. It was developed in stages over the past 30 years as the TGCM (Dickinson et al., 1981; Roble and Ridley, 1987), TIE-GCM (Richmond et al., 1992), and was extended to the middle atmosphere as TIME-GCM by Roble and Ridley (1994) and Roble (1996, 2000). The version used here, known as TIME-GCM version 1.2 which extends vertically from the 10 HPa pressure level (about 30 km) to 5×10^{-10} HPa (~500-700 km depending on solar and geomagnetic activity) with spatial resolution of 5° in latitude and longitude and 2 grid points per scale height. The model time-step is 5 minutes.

2.2 Eddy diffusion. Eddy diffusion plays a large part in controlling the neutral gas composition – in particular the O/N_2 ratio – and it is difficult but important to compute it correctly. In earlier models eddy diffusion was specified throughout the MLT region, but in TIME-GCM-1.2 it is calculated from the flux of gravity waves transmitted upward through complex wind distributions from the base of the model to the turbopause. It uses a modified Lindzen(1981) gravity wave parameterization as described in the

NCAR CCM3 website (http://www.cgd.ucar.edu/cms/ccm3). Increasing the eddy diffusion coefficient causes more O to be transported downward and more N_2 upward, thereby decreasing the ratio of O to N_2.

Gravity wave breaking varies between summer and winter. Wave activity is stronger in winter, particularly in the southern hemisphere, and this variation in gravity wave forcing produces a seasonal variation of the eddy diffusion coefficient about its global mean, the winter value of the eddy diffusion coefficient being 2.5 times larger than in summer.

In order to make the model global mean structure of the O/N_2 ratio consistent with the global mean composition of MSIS-2000, the thermospheric neutral composition - in particular the O/O_2 ratio - has been adjusted by reducing the eddy diffusion coefficient from 90 $m^2 s^{-1}$ to 45 $m^2 s^{-1}$. This adjustment is only for the global mean: the latitudinal, longitudinal and time variations are specified by gravity wave breaking according to the 'Lindzen scheme' as modified by the NCAR CCM3 community model.

2.3 Forcing at the lower boundary. At its lower boundary at the 30 hPa pressure level, about 28 km height, the model is forced at 24-hour intervals with the NCEP global meteorological data. The zonal and meridional winds calculated from the NCEP geopotential height data at the lower boundary set the planetary wave structure around the globe. On them are superimposed the diurnal and semidiurnal propagating tides derived from the Global Scale Wave Model (GSWM) of Hagan et al. (1999) and a specified flux of gravity wave forcing as described above.

2.4 Solar, geomagnetic and ionospheric inputs. TIME-GCM-1.2 is driven with the daily solar F10.7 flux, 81 day average F10.7 cm flux, and geomagnetic Kp imposed every 3 hours. The solar input uses an empirical solar EUV and UV flux model of Solomon and Qian (2005), and the auroral particle input uses the high latitude ion convection model of Roble and Ridley (1987). Plasma flow through the upper boundary still presents an unsolved problem; as in our previous work, we assume an empirical flux of 10^8 cm^{-2} s^{-1}, up by day and down by night. Some ionospheric parameters have been updated from those used in Mendillo et al. (2002), and the model of E-layer electron density has been improved by adjusting the low wavelength EUV (<10 nm) and X-ray flux with the aid of newer satellite data (Solomon et al., 2001).

2.5. Auroral oval model. The auroral oval used in TIME-GCM-1.2 shows both Hobart and Port Stanley well north of the equatorward edge of the auroral oval at local noon, which is 02 UT at Hobart and 16 UT at Stanley. This is as it should be, as Port Stanley is in the 'Weddell Sea anomaly', a region of complex behaviour (Bellchambers and Piggott, 1958; Burns et al., 2008).

3. Results for F2-layer peak electron density

3.1 Solar and geomagnetic conditions for year 2002. The solar-geophysical parameters for the year 2002 are plotted in Fig. 1. The daily solar 10.7 cm flux (top) declined overall during the year from near solar maximum conditions at the beginning to solar medium conditions towards the end, with large 27-day variations caused by localized active regions on the Sun's disk. The lower panels show the daily values of Ap and the numerically greatest values of |Dst| occurring on each day. The geomagnetic indices are typical of solar maximum conditions with equinoctial maxima in April and October.

3.2 How the peak electron density NmF2 varies with local time.

The comparison of daily model output with observations over a full year at multiple stations requires a concise graphical format. We show in Fig. 2 by the red shading how the observed monthly mean for NmF2 ±σ (1 standard deviation) varies diurnally. The daily patterns from the model are shown by the superimposed black curves. Only six sites are shown here and in later figures, Moscow being omitted as the results are similar to those for Chilton, but less complete in data. This format enables an assessment of both the shapes of the diurnal curves as well as their absolute magnitudes. The impression, visually, is that there are far more overlapping regions in the diurnal and seasonal domains between the red (data) and black (model) patterns than there are widely separated characteristics.

In Table 1 we summarize qualitatively on how well TIME-GCM-1.2 represents the shapes of these curves. In Fig. 3, we give the station results for local noon (with the same colour-coding of red for data and black for model output) to portray seasonal effects at a time of day when photochemical equilibrium might be expected to dominate morphologies. In the lower panels for each station, the model output for the O/N_2 ratios are given. In Table 2, we summarize the main features of the variations of noon NmF2 shown in Fig. 3. In both Tables 1 and 2, the seven sites are listed in decreasing order of geographic latitude. Day numbers are quoted in the descriptions to the nearest 5 or 10 (with names of months added in places, for convenience). Labels *near* and *far* refer to the distance in longitude from the meridian of the magnetic pole in the same hemisphere, as in Rishbeth (1998). Tables 1 and 2, collectively, describe overall success of a global model when sampled at specific sites, as well as significant shortfalls during specific times and seasons.

The benefit of a coupled model is that drivers of resultant patterns can be identified. For example, comparing the upper and lower panels for each site in Fig. 3 shows that the variations of O/N_2 ratio bear a strong resemblance to those of NmF2. Additional (but more minor) controlling factors that occur must be related to other atmospheric (dynamical) parameters. Finally, we do not discuss storm conditions when very low NmF2 values appear in the model on some days (e.g., at Wallops Island in September and October in Figure 2), nor nighttime increases due to auroral activity in the model (e.g., at Hobart in April and May), other than to note that significant storm activity occurred during those months (see Fig. 1).

3.3 Midnight F2 layer peak densities. Using the same format as in Fig. 3, we present in Fig. 4 the night-by-night variation throughout the year of peak electron density NmF2 at local midnight, comprising any residual daytime ionization and contributions from the assumed downward flux of oxygen ions. The first thing to note is that there is a pronounced semi-annual effect in the model for all six sites, with no such patterns in the data for the four northern hemisphere sites, and only weak evidence in the southern hemisphere. For Chilton, Eglin, Hobart and Port Stanley, there is no clear correspondence between NmF2 and the O/N_2 ratio in the model, and only a hint of it at Wakkanai and Wallops Island. This is in marked contrast to daytime conditions in the model (Fig. 3). Clearly, the lingering effects of photochemistry are not the drivers of nighttime behaviour; dynamical processes are more important. For absolute magnitudes, the two sites in the southern hemisphere offer the best agreement, and these only due to the weak semi-annual pattern. At present we have no general explanation of the behaviour at midnight, and we have yet to study the data at local times either side of midnight.

3.4 Seasonal and hemispheric patterns. It has long been recognized that the annual pattern of NmF2 and the total electron content of the ionosphere do not follow the simple variations of solar zenith angle throughout the year. While all diurnal patterns for NmF2 clearly show the strong effects of sunrise and sunset, the seasonal variation during midday hours does not follow solar zenith angle. The so-called *Seasonal Anomaly,* as evident in Figs. 2 and 3, refers to the fact that at mid-latitudes daytime NmF2 is larger in local winter than in local summer, in obvious contrast to what might be expected from the variation of solar photo-ionization. This effect occurs in both hemispheres and it therefore helps to validate global models, though in many regions the semiannual variation is stronger.

We select for this aspect of our study the pair of stations Wallops Island and Hobart. These sites have comparable geographic and geomagnetic latitudes and thus are good options for examining possible hemispheric differences in seasonal behaviour. In Fig. 5 we show observations for the summer and winter months of 2002 at both sites. The four-month period May-August is used to portray summer at Wallops Island and winter at Hobart, and the months November-February are winter at Wallops and summer at Hobart (unfortunately, of these four months only January and February 2002 had ionosonde data at Hobart). Nevertheless, in panel (a), the average diurnal curves for summer conditions are very similar with standard deviations clearly overlapping. In panel (b) the four-month averages for winter conditions show a marked difference, the winter ionosphere being more robust in the northern hemisphere. Panel (c) shows the winter/summer ratio for both sites, with about a factor of 2 difference for daytime values.

For model output, we do the same analysis and include the O/N_2 ratio as an aid to interpretation. In Fig. 6, panel (a) gives the summer results, panel (b) the winter results, and panel (c) the winter/summer ratio. The mean diurnal curves for local summer are very similar except for somewhat higher values during the 15-20 LT period at Wallops Island. For local winter, both sites are nearly identical. These attest to comparable physical processes acting in both hemispheres in the model. Fig. 7 shows that the O/N_2 ratios indeed do not differ significantly during daytime hours for these seasons in each hemisphere; the slight differences in the O/N_2 ratio probably arise from different thermospheric circulation patterns.

The most significant effect found in this analysis of seasonal-hemispheric patterns is that the seasonal anomaly is far stronger in data (Fig. 5(c) gives the ratio at ~2.5) than in the model (Fig. 6(c) gives the ratio at ~2). Moreover, the northern hemisphere dominates with the observations (Fig. 5(c)), while the southern hemisphere dominates in the model (Fig. 6(c)). Observationally, this type of behaviour has been known for some time, and is sometimes described as the Annual Asymmetry, with the December-January solstice having a more robust overall ionosphere than the June-July solstice. Rishbeth and Müller-Wodarg (2006) reviewed this topic in some detail and concluded that the models then current could not account for it. Recent model studies by Qian et al. (2008) have successfully reproduced seasonal and semi-annual variations in thermospheric densities by adjusting the eddy diffusion coefficient to have a global annual variation. Additional analyses are needed to see if these new results apply equally well to ionospheric densities.

4. Calibration of the TIME-GCM 1.2 ionospheric model at noon.

Having assessed the shapes of diurnal patterns, seasonal effects and the annual asymmetry, we now offer an overall view of how data and model output compare in absolute values. Table 4 shows the model/data ratios of noon NmF2 expressed as natural (base e) logarithms. Minus signs imply that model values are less than the ionosonde values. Omitting Moscow because of four missing months, the average for the remaining four northern sites is 0.20 which corresponds to a factor of 1.22, and for the two southern sites it is 0.27 which corresponds to a factor of 1.31. This means that model values of NmF2 are on average 27% high, which may be claimed as remarkably accurate given all the difficulties inherent in a global model. For the northern hemisphere, where we have conducted more station comparisons, the model may be regarded as well calibrated, though many individual values in the table exceed 0.3 which corresponds to a factor of 1.35, i.e., model values are 35% high. At months and sites with large factors, such as during days 180-270 (July-September) at Wakkanai, Hobart and Port Stanley, these appear to arise for different reasons. For example, at Wakkanai the model gives wrong day-by-day shapes with too pronounced a diurnal variation, perhaps indicative of thermospheric circulation problems in the model. At Hobart and Port Stanley, the diurnal shapes are acceptable but are simply too high in magnitude, again suggestive of O/N_2 issues.

5. Discussion.

5.1 General. The conclusion from sections 3 and 4 is that at noon the 1.2 version of the TIME-GCM model represents very well the '1-365' day-by-day variation of peak electron density NmF2 at the northern mid-latitude sites, except for a few individual sites and months. In the southern hemisphere, the months July-September notably over-estimate magnitudes during the daytime, as also occurs at some northern sites. Interestingly, these 2002 months of southern hemisphere winter and spring included three large 27-day solar rotation effects, as shown in panel (a) for Fig. 1. The strong photo-production results in the model for these periods may have been caused via the F10.7 parameterization scheme of solar irradiance in the model, affecting each hemisphere somewhat differently, as occurs with the seasonal anomaly. Moreover, southern hemisphere winter in 2002 had very large planetary wave activity and the first ever major stratospheric warming during September and October documented in that hemisphere. Liu and Roble (2002, 2005) have addressed this issue in some detail. Perhaps the model produces too large of a coupling from below from NCEP data during these events, ultimately affecting the photo-chemistry of the F-layer in that hemisphere.

At midnight, the model (with its assumed flux of O^+ ions from above) gives overall patterns in the southern hemisphere that are quite good. Except for strong peaks of NmF2 during the equinoxes at all four northern hemisphere sites, which are not seen in the data, the model gives acceptable representations of the nighttime F2-layer absolute density values.

5.3 Vertical flow of the neutral air. Fig. 8 illustrates the general pattern of upwelling and downwelling of the neutral air, envisaged by Duncan (1969) and computed by Rishbeth and Müller-Wodarg (1999), with a downwelling zone at moderately high winter latitudes but equatorward of the winter auroral oval. Though we have not investigated vertical velocities in this paper, this pattern is consistent with the idea that the O/N_2 ratio is influenced by vertical velocity. This is shown in various model results, e.g., ratios ranging from 3-9 are common for successful daytime patterns shown in figures 3 and 7. Observationally, the high winter NmF2 at the northernmost sites (e.g., red-coded data points in Dec-Jan at Chilton in Fig. 3) imply that they lie within the downwelling zone, while the more modest winter NmF2 at the southern sites, Hobart and Port Stanley (red-coded data points in June-July in Fig. 3), imply that the downwelling zone usually lies to their south, though day-to-day changes at these sites suggest that the zone sometimes moves far enough north to include them. In a previous study using other ionosonde sites, the rather high winter NmF2 at Kerguelen in the South Indian Ocean at 49°S, 70°E (Zou et al., 2000) imply that the downwelling zone normally includes that site. Furthermore, perusal of three solar cycles of midwinter (June) data from Faraday, in the Antarctic peninsula at 65°S, 64°W, shows that monthly mean NmF2 lies in the range 2-8 x 10^5 cm^{-3} at noon (higher than might be expected with the noonday sun virtually on the horizon), which suggests that the downwelling zone may even extend far enough south to include Faraday. Another global circulation model, CTIPM (Zou et al., 2000), portrays fairly well the month-to-month variations of NmF2 at Hobart, Port Stanley and Kerguelen, implying that it uses a satisfactory model of the southern auroral oval and hence the source circulation from high latitudes.

5.3 Day-to-day variability. While the focus of this paper is the correct representation of diurnal, seasonal and hemispheric behaviour of the F2-layer peak electron density, the set of comparisons given in Fig.2 contain information about patterns of variability. In each panel, the shading gives the observed monthly mean NmF2 ± the standard deviation of the mean for each hour (typically 20-25%). For an ideal distribution about the mean, two-thirds of the observed diurnal curves would fall within the shading. The curves shown, however, are from the model, and thus one can get a preliminary feel about the ability to simulate day-to-day fluctuations using TIME-GCM-1.2. For example, there are station-months where virtually all of the model curves fall within the red shading (June at Chilton, January at Hobart), implying an under-portrayal of variability. The opposite occurs at other station-months (e.g., January at Eglin and July at Port Stanley) where the model's variability exceeds those from observations. With all three sources of variability on during these runs of TIME-GCM-1.2 (solar, geomagnetic and meteorological), we are unable to point to the contribution factors from each source. We intend to discuss this fully in a subsequent paper, noting here only the obvious fact that daily inputs from these three sources of variability do indeed result in marked day-to-day changes in the model output.

6. Conclusion.

The TIME-GCM-1.2 coupled model reproduces midday NmF2 well throughout year 2002 at seven mid-latitude sites. The variations of O/N_2 ratio near the F2 peak follow a similar pattern, strongly supporting the idea that NmF2 is linked to the chemical composition of the ambient neutral air. At midnight the model is more successful in the southern hemisphere, with the model predicting strong equinoctial peaks in the northern hemisphere that are not seen in the data.

Section 4 discussed the absolute values of NmF2, month by month and site by site, arriving at an overall 'calibration factor' of 1.27. This implies that the model values exceed observed values on average by 27%, a quite accurate performance. The atomic/molecular concentration ratio is affected by eddy diffusion, which we have adjusted according to the best available information, and by the pattern of vertical motions ('upwelling' and 'downwelling') of the neutral air. This implies that getting these processes right is necessary for good F2 layer modelling. It is encouraging that the model reproduces the seasonal and semiannual variations of NmF2 quite successfully. We expect to use the improved modelling achieved via this validation as the basis for future work in which different forcings at the upper and lower boundaries will be imposed.

Rishbeth and Mendillo (2001) found that recorded values of NmF2 at several ionospheric sites show considerable day-to-day variability that occurs in differing episodes at different sites. They surmised that this component of variability stems from the variable forcing by dynamic processes, generated in the lower atmosphere and propagated to the ionosphere as mutually interacting planetary waves, tides and gravity waves. We intend to conduct a future study using TIME-GCM-1.2 to explore the contributions of coupling from below using NCEP sources for coupling from the lower atmosphere, together with solar and geomagnetic input, and then with the TIME-GCM-1.3 with the European Centre for Medium-range Weather Forecasts (ECMWF) model for input from below.

Other topics for future discussion are the problems posed by (1) the day-to-day variability of the height of the F2-peak electron density, (2) the differences of NmF2 between the March and September equinoxes, (3) the seasonal variation of thermospheric temperature, with maxima shortly after the equinoxes, (4) the semiannual variation of F2 peak height hmF2 which is closely related to (3), and (5) the continuing necessity for an assumed downward flux at night. Up to now, TIME-GCM and other coupled models have failed to resolve these well-established questions, and we have yet to see critical discussion of all five. We believe our day-to-day modelling of data for an actual year (2002) represents a significant advance. Thermospheric modelling is not complete, but it has come a long way!

Acknowledgments

We are most grateful to Ben Foster for his assistance with the TIME-GCM calculations and for providing model output for comparison with ionosonde data, and to Alan Burns for the use of his model of the auroral ovals. We thank the World Data Centres A and C1 for Solar-Terrestrial Physics at Boulder, Colorado, and Chilton, UK, for supplying data. At Boston University, support for this study was provided in part by a grant from the Aeronomy Program of the US National Science Foundation (NSF). The National Center for Atmospheric Research is sponsored by the US National Science Foundation.

References

Bellchambers, W. H., Piggott, W. R., 1958. Ionospheric measurements made at Halley Bay. Nature 182, 1596-1597.

Burns, A. G., Z. Zeng, W. Wang, J. Lei, S.C., Solomon, A. D. Richmond, T. L. Killeen, and Y.-H. Kuo, The behaviour of the F2 peak ionosphere over the South Pacific at dusk during quiet summer conditions from COSMIC data. Journal of Geophysical Research (submitted), 2008.

Dickinson, R. E., Ridley, E.C., Roble, R. G., 1981. A three-dimensional general circulation model of the thermosphere. Journal of Geophysical Research 86, 1499-1512.

Duncan, R. A., 1969. F-region seasonal and magnetic storm behaviour. Journal of Atmospheric and Terrestrial Physics 31, 59-70.

Forbes, J. M., Palo, S. E., Zhang, X, 2000, Variability of the ionosphere. Journal of Atmospheric and Solar-Terrestrial Physics 62, 685-693.

Fuller-Rowell, T. J., Codrescu, M., Wilkinson, P., 2000. Quantitative modelling of the ionospheric response to geomagnetic activity. Annales Geophysicae 18, 766-781.

Hagan, M. E., Burrage, M. D., Forbes, J. M., Hackney, J., Randel, W. J., Zhang, X., 1999. GSWM-98: Results from migrating solar tides, Journal of Geophysical Research 104(A4), 6813-6828.

Lindzen, R. S., 1981. Turbulence and stress owing to gravity wave and tidal breakdown, Journal of Geophysical Research 86, 9707-9714.

Liu, H.-L., Roble, R. G., 2002. A study of a self-generated stratospheric sudden warming and its mesospheric/lower thermospheric impacts using coupled TIME-GCM/CCM3, Journal of Geophysical Research 107(D23), 4695, doi:10.1029/2001JD001533.

Liu, H.-L., Roble, R., 2005. Dynamical coupling of the stratosphere and mesosphere in the 2002 Southern Hemisphere major stratospheric sudden warming, Geophysical Research Letters 32, L13804, doi:10.1029/2005GL022939.

Mendillo, M., Rishbeth, H., Roble. R. G., Wroten, J., 2002. Modelling F2-layer seasonal trends and day-to-day variability driven by coupling with the lower atmosphere. Journal of Atmospheric and Solar-Terrestrial Physics 64, 1911-1931.

Picone, J. M., Hedin, A. E., Drob, D. P., Aikin, A. C., 2002. NRLMSISE-00 empirical model of the atmosphere: statistical comparisons and scientific issues. Journal of Geophysical Research 107 (A12), 1468, doi:10.1029/2002JA009430.

Qian, L., S. C. Solomon, and T. J. Killeen, 2008, Seasonal variation of thermospheric density and composition, Journal of Geophysical Research (in press).

Richmond, A. D., Ridley E.C., Roble, R.G., 1992. A thermosphere/ionosphere general circulation model with coupled electrodynamics. Geophysical Research Letters 19, 601-604.

Rishbeth, H., 1998, How the thermospheric circulation affects the ionospheric F2-layer. Journal of Atmospheric and Solar-Terrestrial Physics 60, 1385-1402.

Rishbeth, H., Mendillo, M., 2001. Patterns of ionospheric variability. Journal of Atmospheric and Solar-Terrestrial Physics 63, 1661-1680.

Rishbeth, H., Müller-Wodarg, I.C.F., 1999. Vertical circulation and thermospheric composition: a modelling study. Annales Geophysicae 17, 794-805.

Rishbeth, H., Müller-Wodarg I. C. F., 2006. Why is there more ionosphere in January than July? The annual asymmetry in the ionospheric F2-layer. Annales Geophysicae 24, 3293-3311.

Roble, R. G., 1996. The NCAR Thermosphere Ionosphere Mesosphere Electrodynamics General Circulation Model (TIME-GCM). In: Schunk, R. W. (Ed.), STEP Handbook of Ionospheric Models. Utah State University, pp. 281-288.

Roble, R.G., 2000. On the feasibility of developing a global atmospheric model extending from the ground to the exosphere. Geophysical Monograph, Vol. 123, American Geophysical Union, Washington DC, pp. 53-67.

Roble, R. G., and E.C. Ridley, 1987. An auroral model for the NCAR thermosphere general circulation model (TGCM). Annales Geophysicae 5A, 369-382.

Roble, R. G., and E.C. Ridley, 1994. A thermosphere–ionosphere–mesosphere–electrodynamics general circulation model (TIME-GCM): equinox solar cycle minimum simulations (30–500 km). Geophysical Research Letters 21, 417-420.

Solomon, S. C., Bailey, S. M., Woods, T. N., 2001. Effect of solar soft X-rays on the lower ionosphere. Geophysical Research Letters 28, 2149.

Solomon, S. C., and Qian, L. 2005. Solar extreme-ultraviolet irradiance for general circulation models. Journal of Geophysical Research, 110, A10306, doi:10.1029/2005JA11160.

Zou, L., Rishbeth, H., Müller-Wodarg I. C. F., Aylward, A.D., Millward, G.H., Fuller-Rowell, T.J., Idenden, D.W., and Moffett, R.J., 2000. Annual and semiannual variations in the ionospheric F2-layer:I. Modelling, Annales Geophysicae 18, 927-944.

511 **Table 1 Comments on shapes of daytime variations of NmF2 vs time (Fig. 2).**

Moscow 56°N 37°E	Model shapes are very good on the whole, but omit the forenoon peaks (08-10 LT) in spring, especially April. Magnitudes also very good, with only February and September slightly high.
Chilton 52°N 2°W	Very much as for Moscow, with excellent agreement overall.
Wakkanai 45°N 142°W	Model shapes match the data badly. In the winter half of the year (Jan-Apr, Sept-Dec), the diurnal maxima occur several hours later than observed. In summer, the model fails to capture the flat daytime pattern versus local time.
Wallops Is 39°N 77°W	In many months the shapes match well, but the afternoon peaks tend to occur later in the model than in the data, especially near the equinoxes.
Eglin 30°N 87°W	Daytime peaks in the model occur 2-4 hours too late in every month. The flat diurnal pattern during daytime in summer (Jun-Aug) is not captured in the model.
Hobart 43°S 147°E	Model shapes match the data quite well, though with bad mismatches in actual values during winter and spring months.
P Stanley 52°S 58°W	The daytime peaks from the model mostly occur 2-4 hours too late, and in southern winter the model/data mismatch in absolute values is very prominent.

512

Table 2 Comparisons of model with data for noon NmF2 (Fig. 3).

Label *near* and *far* refer to longitude distance from the meridian of the magnetic pole.

Moscow 56°N *near*	No data June or Oct-Dec (days 150-180, 270-365). Very good agreement except during early spring (days near ~45) when model values are ~25% too high in magnitude.
Chilton 52°N *near*	Excellent agreement throughout the year. As with Moscow, model slightly high during February.
Wakkanai 45°N *far*	Data values peak at days 30-35 (Feb) and 300-330 (Nov). Model values are good in late spring and fall, but again too high in February and for days 200-300 (July-Sept).
Wallops Is. 39°N *near*	Data values are surprisingly flat Jan to early Apr (days 1-100), but model shows Feb maximum around days 40-45. Model fits data well rest of year, but is slightly too high in late summer.
Eglin 30°N *near*	No data days 225-260 (Aug-Sept). Fairly good fit overall, but model under-portrays the winter to summer ratio (Jan to July).
Hobart 43°S *near*	No data days 305-365 (Nov-Dec). Model values are good on days 1-110 (Jan-Apr) and then slightly high to mid-year, but much too high throughout late winter and spring (days 200-300). The data show weak semi-annual peaks near the equinoxes, while the model over-portrays the late winter/spring maximum.

P Stanley 52°S *far*	Data show a basic semi-annual variation, peaking in autumn at days 90-100 (April) and in spring (days 260-310, Sept-Oct). In the model, a strong semi-annual variation is present, with the first peak advanced slightly in comparison to the data, but with the second peak occurring early by more than a month. The absolute values are thus too high in the model from June to September.

Table 3 **Comparisons of model and data for midnight NmF2 (Fig. 4).**

Labels *near* and *far* refer to longitude distance from the meridian of the magnetic pole.

Moscow 56°N *near*	No data June or Oct-Dec (days 150-180, 270-365). Data show flat peak in summer (days 80-210), tailing off towards day 270 (late Sept). Model values show semi-annual (equinoctial) peaks well above observations.
Chilton 52°N *near*	Data are very similar to Moscow (and more complete) with flat peak in early summer (days 70-190) tailing off towards day 270 (late Sept). Model values are too high throughout the equinox months, showing a pronounced semi-annual variation not in the data.
Wakkanai 45°N *far*	Data show a summer plateau, days 100-280 (Apr-Oct). Model values are strongly semi-annual, with serious mis-match with data for most of year.
Wallops Is. 39°N *near*	Data are rather flat throughout year, slightly raised at days 110-230 (Apr-Aug) with many individual values showing nighttime increase effects. Model values flat during summer with good agreement in absolute value with data. Model has marked Feb-Mar and Oct peaks in very poor agreement with observations.
Eglin 30°N *near*	Data very similar to Chilton and Wakkanai. They rise sharply days 1-90, peak in early summer at days 120-150 (May), slowly decline during days 150-310 (June-Oct), stay flat till year end. Model variation very similar to Wakkanai with strong semi-annual pattern not seen observationally.

Hobart 43°S *near*	No data days 305-365 (Nov-Dec). Data show nearly flat winter minimum (days 140-220). Model values again semi-annual showing best agreement in absolute magnitude among the seven stations. Model values above data during late winter and spring.
P Stanley 52°S *far*	Data peak in late summer (days 10-30) and in early summer (days 310 340), sloping down in autumn to flat minimum in winter (days 150-200) and sloping up in spring. Model values match overall magnitudes well, but with seriously different pattern dominated by semi-annual variation not in data.

Table 4. Month-by-month calibrations between model and data.

Each entry gives the monthly average of the daily ratios, expressed as the natural log of noon NmF2 (model)/NmF2 (data). For southern hemisphere, overall average is expressed in two ways due to no data from Hobart for two months of 2002.

	Chilton	Wallops	Wakkanai	Eglin		N.H. Monthly Mean
Jan	-0.03	0.18	0.12	-0.45		-0.04
Feb	0.14	0.23	0.24	-0.25		0.09
Mar	0.07	0.20	0.16	-0.20		0.06
Apr	0.04	0.13	0.14	0.03		0.08
May	-0.12	0.36	0.36	0.04		0.16
Jun	0.04	0.27	0.41	0.28		0.25
Jul	0.16	0.53	0.49	0.56		0.44
Aug	0.33	0.63	0.83	0.49		0.57
Sep	0.23	0.42	0.82	0.12		0.40
Oct	0.37	0.16	0.54	0.20		0.32
Nov	0.21	-0.02	0.18	-0.02		0.09
Dec	-0.03	-0.14	0.13	-0.20		-0.06
mean:	0.12	0.25	0.37	0.05	0.20	0.20

	Hobart	P.Stanley		S. H. Monthly Mean
Jan	0.17	-0.28		-0.06
Feb	0.45	-0.20		0.13
Mar	0.20	-0.18		0.01
Apr	0.29	-0.06		0.11
May	0.19	0.32		0.25
Jun	0.29	0.67		0.48
Jul	0.57	0.94		0.76
Aug	0.70	0.90		0.80
Sep	0.52	0.23		0.38
Oct	0.78	-0.38		0.20
Nov		-0.18		-0.18
Dec		-0.26		-0.26
mean:	0.41	0.13	0.27	0.22

Figure Captions

Fig. 1 Daily values of solar F10.7 cm flux and the geomagnetic indices Ap and $|Dst|_{max}$ for 2002, 'max' denoting the numerically greatest value occurring on the UT date.

Fig. 2 NmF2 vs universal time for twelve months at six sites. The black curves are the daily curves computed from the TIME-GCM-1.2 model. The red shading shows the observed monthly mean NmF2 ± 1 standard deviation. Ideally, two-thirds of the model curves should lie within the red shading.

Fig. 3 Noon NmF2 on days 1-365 for six sites: ionosonde data and TIME-GCM-1.2 model output for NmF2 and noon O/N_2 ratio on the pressure level nearest the F2 peak.

Fig. 4 Midnight NmF2 on days 1-365 at six sites: ionosonde data and TIME-GCM-1.2 model, and midnight O/N_2 ratio on the pressure level nearest the F2 peak.

Fig. 5 Average behaviour of observed NmF2 at Wallops Island (VA) and Hobart (Tasmania) for (a) Summer and (b) Winter months, and (c) the Winter/Summer ratio. Shadings in panels (a) and (b) give standard deviations (see text).

Fig. 6 Average behaviour of modelled NmF2 at Wallops Island (VA) and Hobart (Tasmania) for (a) Summer and (b) Winter months, and (c) the Winter/Summer ratio. Shadings in panels (a) and (b) give standard deviations (see text). Note that the ratio in panel (c) is similar at both sites, as modelled, but different from the observed patterns in Fig. 5(c).

Fig. 7 Model results for the atomic oxygen to molecular nitrogen ratio at Wallops Island and Hobart from the TIME-GCM-1.2 run that produced the NmF2 patterns shown in Fig. 6.

Fig. 8 Sketch of the thermospheric circulation, after Rishbeth (1998). The figure represents average conditions in June at around 300 km at no particular longitude. The bold dashed lines at the top and bottom represent the auroral ovals, the dash-dot curve represents the sunrise/sunset terminator, thin dotted lines represent typical isobars, and arrows represent wind directions (but not magnitudes). The upward pointing triangle at 14 LT shows the position of maximum temperature and pressure; the downward pointing triangle at 03 LT shows the position of minimum temperature and pressure. Note that the six hours 00-06 LT are repeated on the right-hand side.

Figure1
Click here to download high resolution image

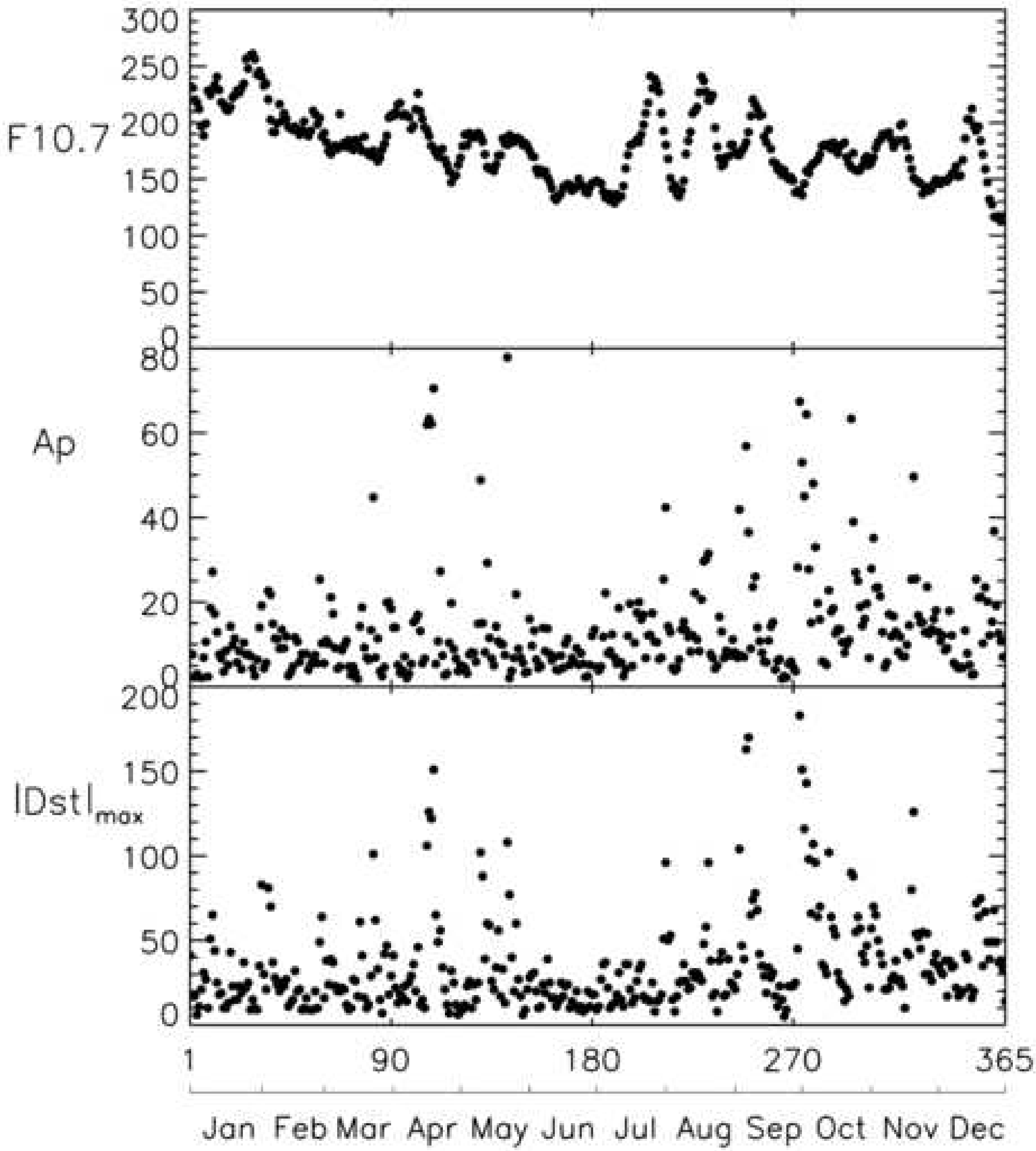

Figure2
Click here to download high resolution image

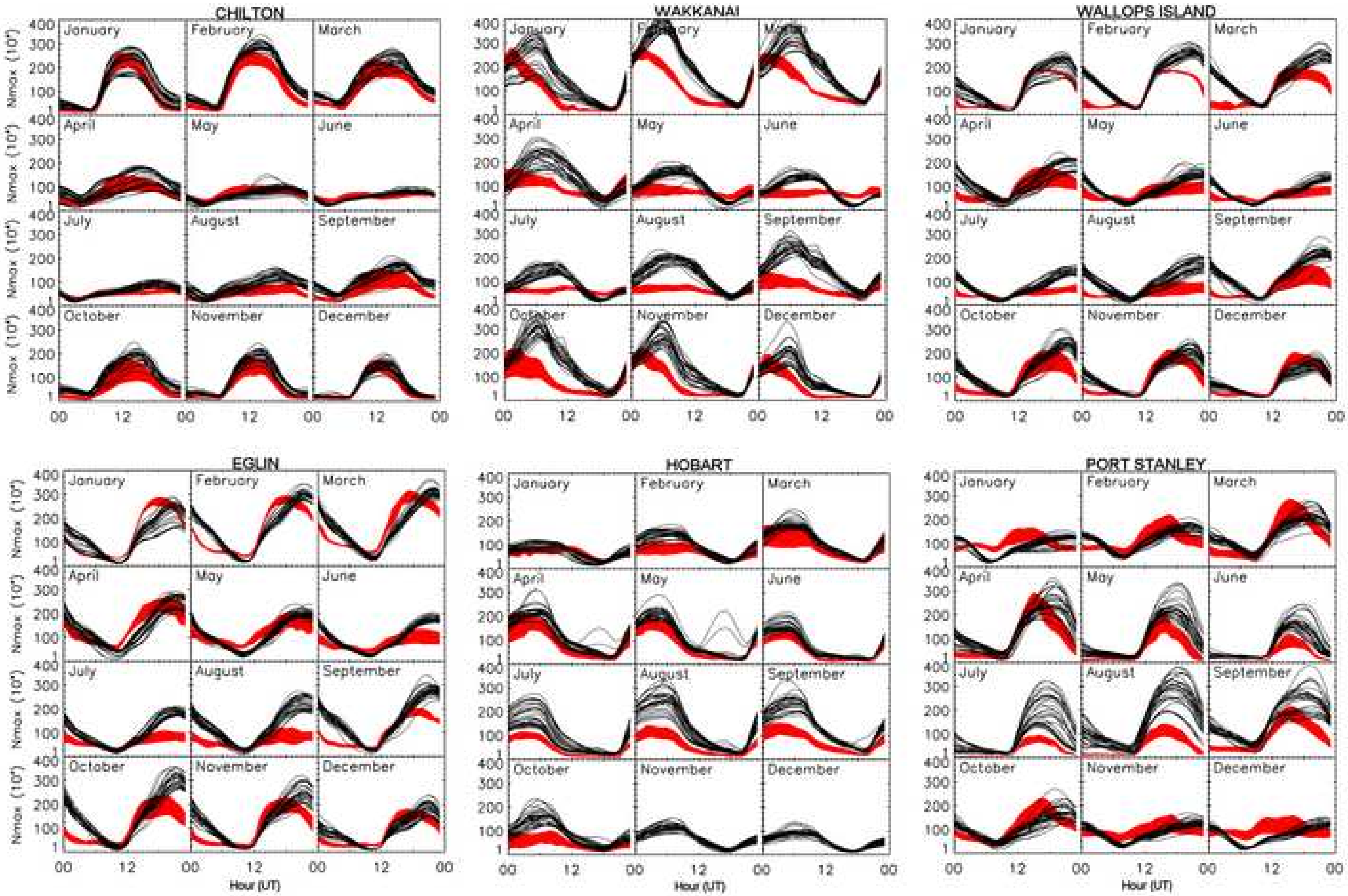

Figure3

Click here to download high resolution image

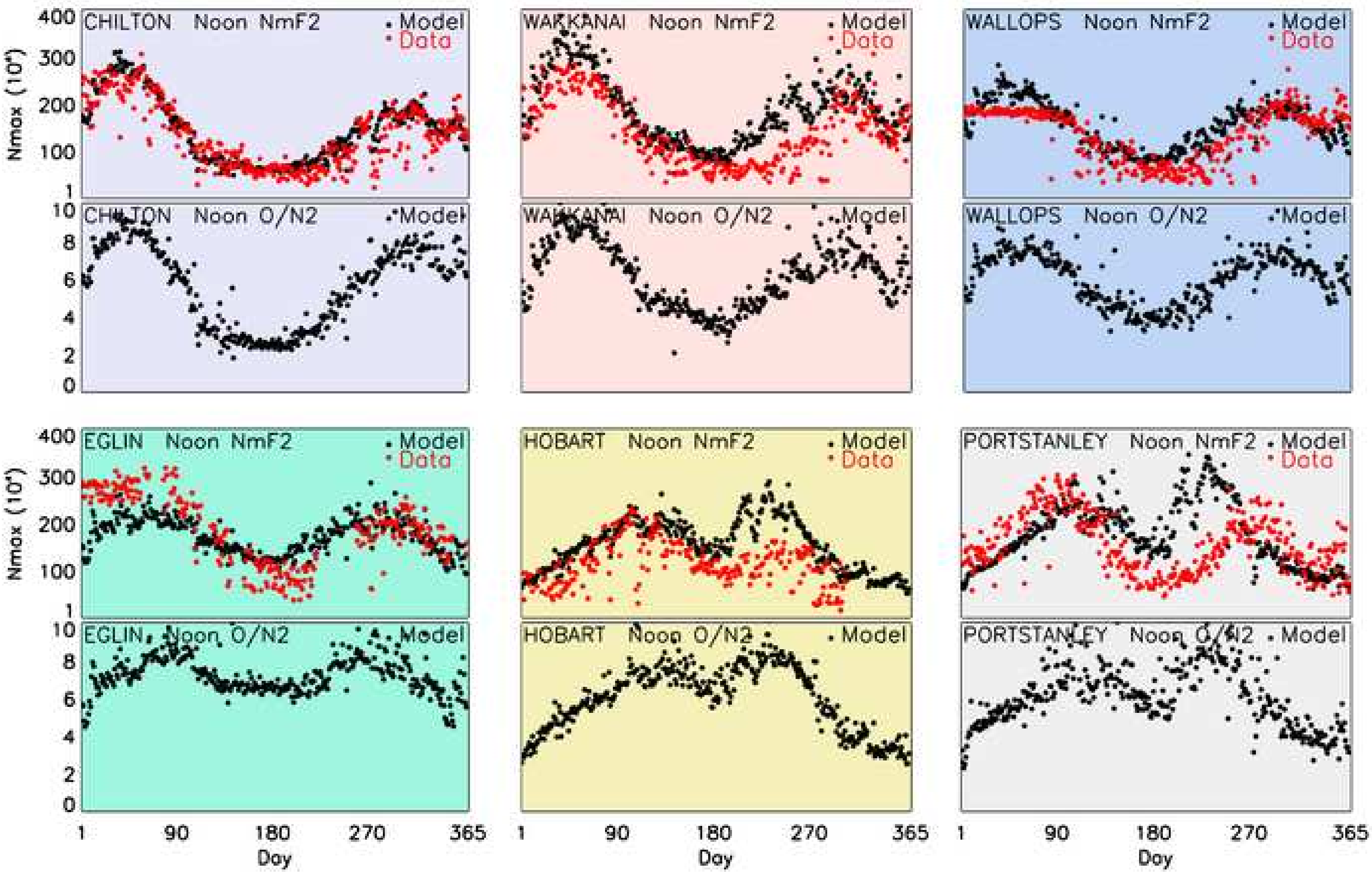

Figure4

Click here to download high resolution image

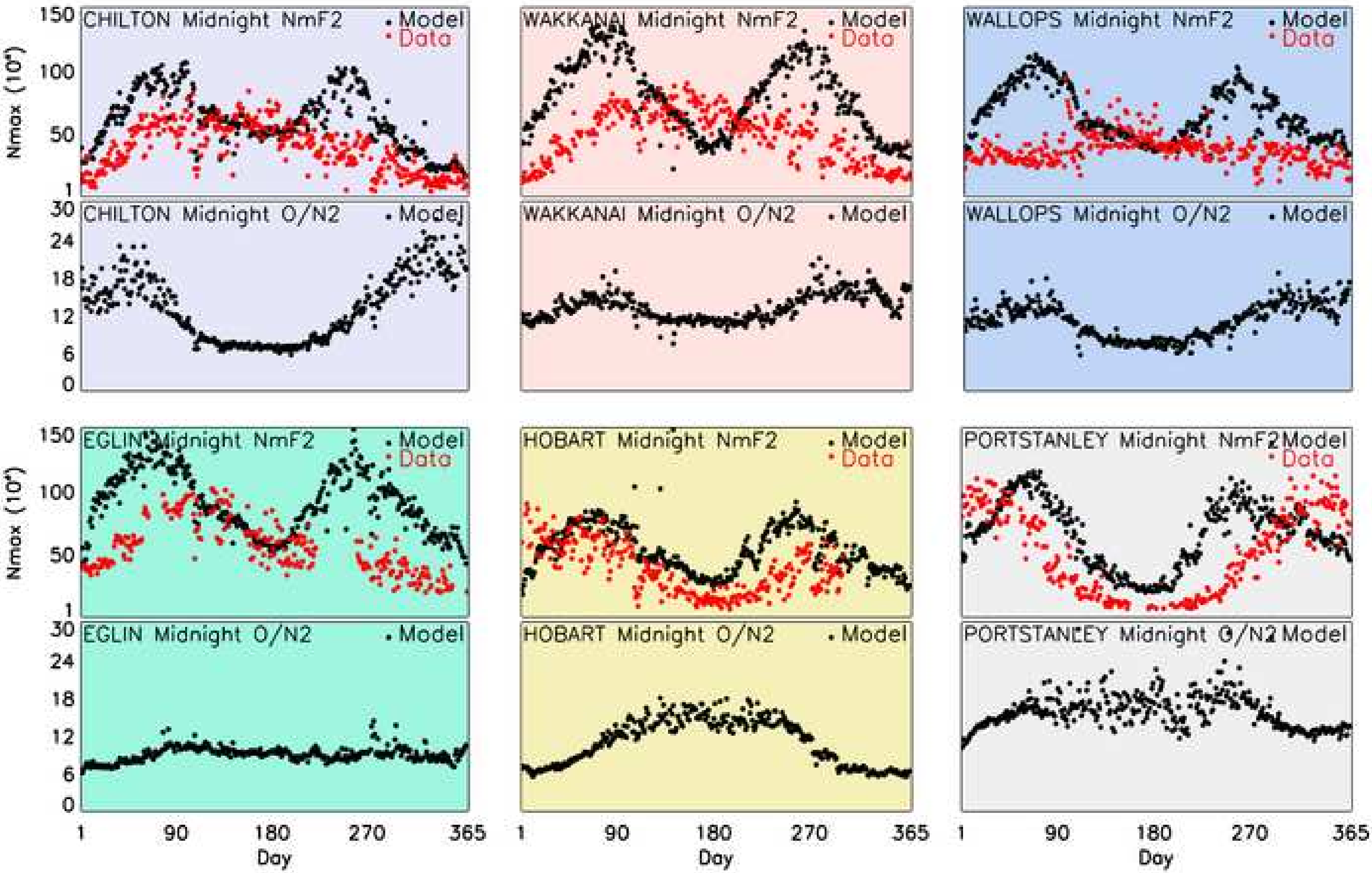

Figure5

Click here to download high resolution image

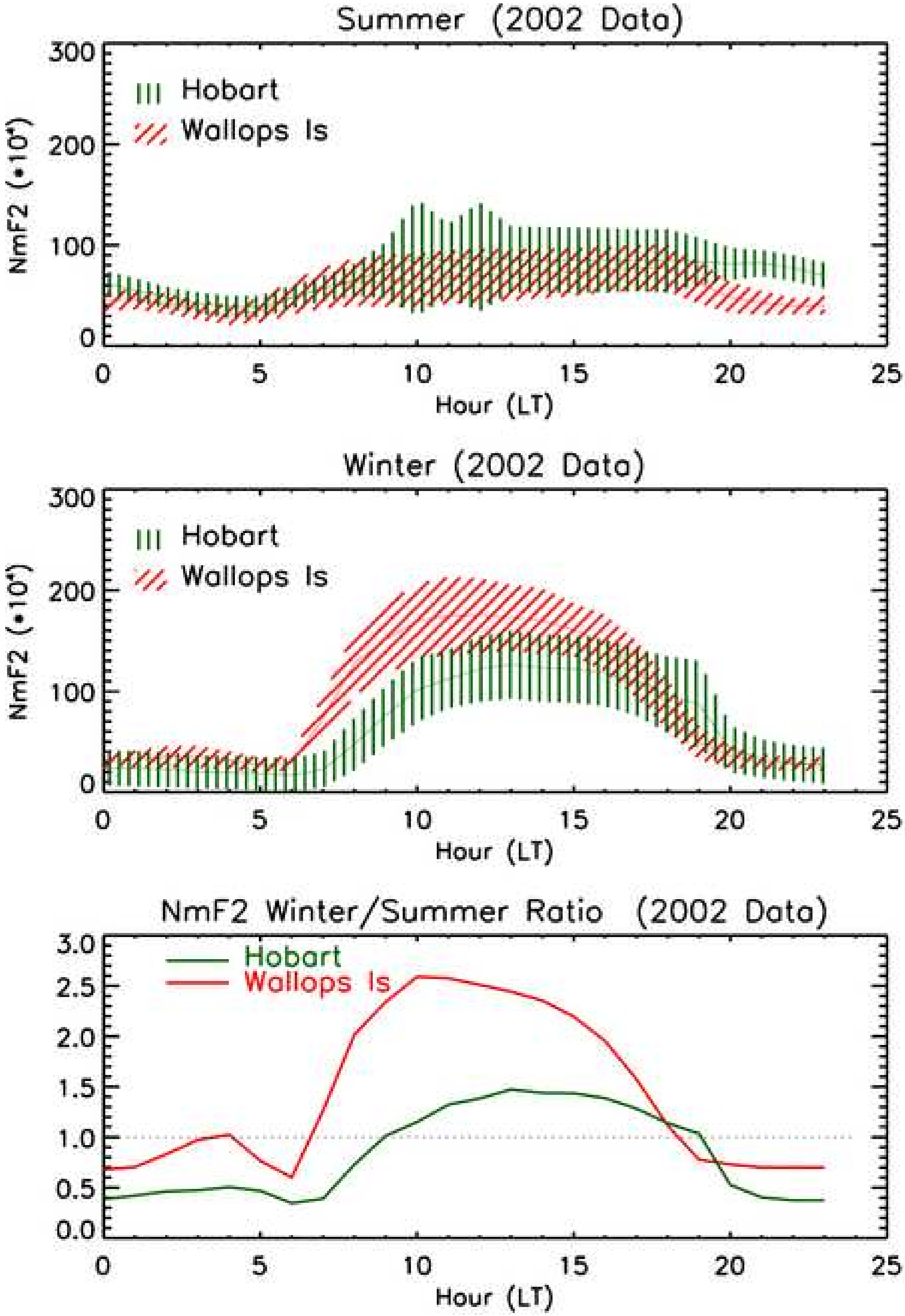

Figure6

Click here to download high resolution image

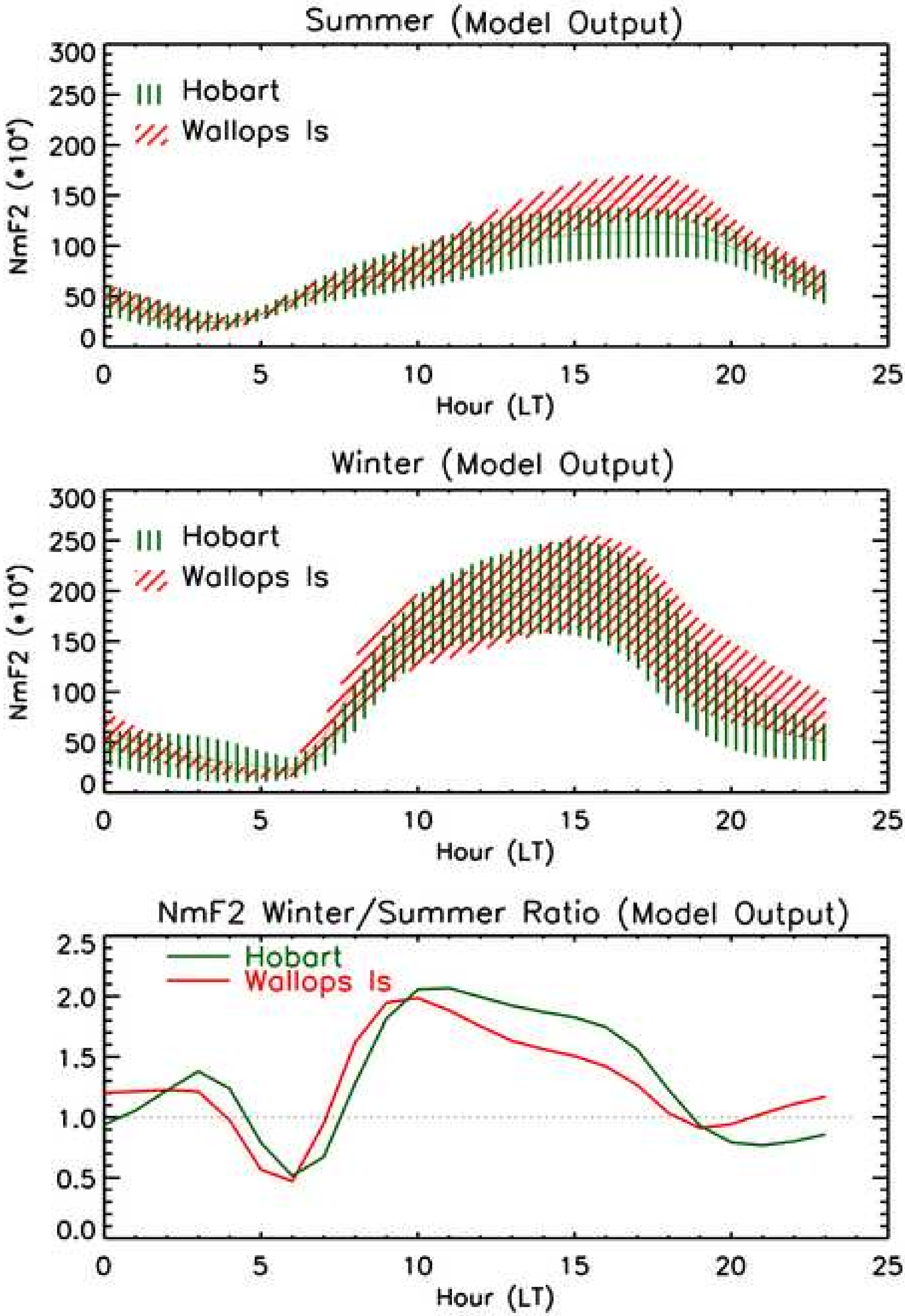

Figure7

Click here to download high resolution image

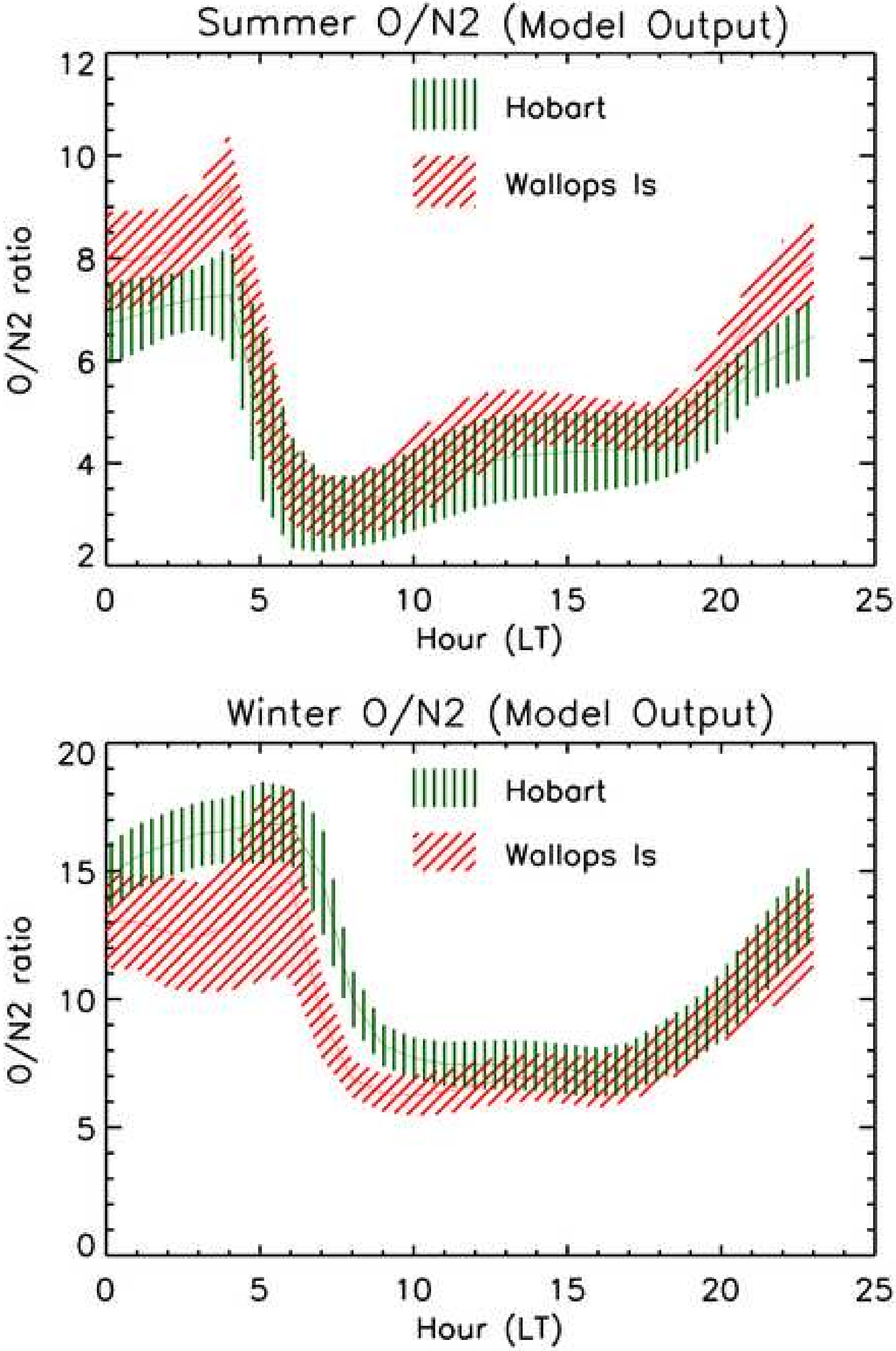

Figure8
Click here to download high resolution image